

Available online at [www.sciencedirect.com](http://www.sciencedirect.com)**ScienceDirect**

Energy Procedia 69 (2015) 208 – 217

---

---

Energy  
**Procedia**

---

---

International Conference on Concentrating Solar Power and Chemical Energy Systems,  
SolarPACES 2014

## Inverse MCRT method for obtaining solar concentrators with quasi-planar flux distribution

J.J. Serrano-Aguilera<sup>a,\*</sup>, L. Valenzuela<sup>a</sup>, J. Fernández-Reche<sup>a</sup>,<sup>a</sup> CIEMAT-Plataforma Solar de Almería, Crta. de Senés, km. 4.5, Tabernas, Almería, E04200, Spain

---

### Abstract

A numerical algorithm has been developed in order to get reflectors geometry so that the desired flux distribution is approximately obtained. This new method opens up the opportunity to design ad-hoc line-focus solar reflectors for a specific purpose from the required concentrated flux distribution. A new design for PTC reflectors is proposed, getting a quasi-planar distribution around the absorber. This algorithm can also be applied not only to round absorbers in PTC applications but others like flat absorbers useful for concentrated solar photovoltaic/thermal systems. The proposed new reflector geometries will be compared to the classical Eurotrough-type parabolic-trough geometry by means of the intercept factor and the tolerance to absorber displacements respect to the design location.

© 2015 The Authors. Published by Elsevier Ltd. This is an open access article under the CC BY-NC-ND license

(<http://creativecommons.org/licenses/by-nc-nd/4.0/>).

Peer review by the scientific conference committee of SolarPACES 2014 under responsibility of PSE AG

**Keywords:** line-focus solar collector; MCRT; Inverse MCRT; radiation flux profile; intercept factor; parabolic-trough

---

### 1. Introduction

Parabolic-trough collector systems are based on parabolic mirrors that concentrate the solar radiation according to a known angular distribution. For the standard design of parabolic troughs available in the market (LS-3 or EuroTrough [1,2,3] geometries), this angular distribution produces two radiation flux peaks and a considerable thermal gradient around the absorber tube for some heat transfer fluid types and fluid flow rate conditions. The

---

\* Corresponding author. Tel.: +34 950 387 800 (ext 905) .

E-mail address: [jserrano@psa.es](mailto:jserrano@psa.es), [jj.serragui@gmail.com](mailto:jj.serragui@gmail.com)

redesign of the reflector geometry leads to get better flux distribution, reducing thermal gradients and others subsequent drawbacks like radiation losses or thermal bending (especially in DSG applications [4]). This last undesirable effect may produce receiver displacements respect to the design location (focal line), causing optical performance reduction and glass envelope breaking risk.

### Nomenclature

CPVT	Concentrating Photovoltaic/Thermal
DSG	Direct Steam Generation
IMCRT	Inverse Monte Carlos Ray Tracing
MCRT	Monte Carlo Ray Tracing
PTC	Parabolic Trough Collector
$N$	number of segments in the reflector discretization
$R_{\text{abs}}$	absorber tube radius
$n$	refractive index
$\Psi$	intersection angle of the ray at the edge
$\theta$	azimuthal coordinate around the absorber
$\theta_{\text{max}}$	constant concentrated radiation flux profile width (one half)
$\Lambda$	relative arc length of the reflector respect to the LS-3 design
$\gamma$	intercept factor
$\delta$	vector direction
$A_{99}$	non-dimensionalised displacement area where the intercept factor is higher than 0.99

Most of CPVT systems have been conceived based on dish concentrators [5]. The idea of implementing CPVT systems based on linear concentrators requires from achieving constant concentrated flux distribution onto the absorber (e.g. flat absorber [6]) containing the photovoltaic cells [7, 8]. This concept has been addressed by means of linear mirror concentrators [9, 10]. This new method provides the chance to modify the PTC reflector geometry so that a quasi-planar radiation flux is obtained to be applied to CPVT purposes.

## 2. Method description

The purpose of the proposed method is to provide numerically the reflector geometry so that its concentrated flux distribution onto the absorber is close to the objective flux distribution required. It is an approximate “Inverse Monte Carlo Ray Tracing Method” (IMCRT) aiming to set the reverse process respect to the classical MCRT methods, where the concentrated flux distribution from any reflector shape is obtained. Despite the fact that we have focused this method on round absorbers (PTC applications) looking for a constant flux distribution around the metallic absorber tube within a predefined angular range, this algorithm can be also applied to get any flux distribution (e.g. triangular flux distributions) or to not round absorbers. Due to the fact that the Sun is not a point source, a realistic sunshape distribution is required. This sunshape distribution provides the probability that every ray (direct solar radiation) is deviated a specific angle respect to the central ray from the Sun (theoretical rays orientation in case of considering Sun as a point source). In this work we have used the experimental sunshape provided by Neumann [11]. Owing to this sunshape profile, we cannot reach the same exact flux distribution that the initially required (specially sharp distributions with steps described by not differentiable functions) but we can get the reflector geometry that approximates reasonably to the objective. This method is formed by two main stages:

- Stage #1: The Sun is considered as a point source. This enables to get a close solution to the required flux distribution. This first solution is the initial guess for the next stage.

- Stage #2: The second step consists of non-linear optimization tasks aiming to correct as much as possible the effects of the sunshape profiles. It is a refinement process in which we modify slightly the reflector geometry to get a closer solution to the objective concentrated-flux distribution.

### 2.1. Stage #1: Initial guess calculation

This first algorithm step aims to provide an approximate first solution to the problem. A numerical approach is taken to tackle this task, so a discretization of the reflector geometry is assumed, describing the reflector geometry as a group of differential connected segments.

The first required information is the objective flux profile; in which we set the needed concentrated flux distribution around the absorber tube. One relevant case is the constant radiation flux profile due to its practical interest. The example shown in Fig. 1(a) concentrates all the incoming solar radiation for the Eurotrough design (aperture length of  $W=5.76$  m) into a constant distribution within the angular range  $(-0.8\pi \leq \theta \leq 0.8\pi)$  around the absorber, assuming the absorber radius as  $R_{abs}=0.035$  m. Apart from the objective profile we aim to get, it is necessary to set the intersection angle  $\Psi$  (see Fig. 1(b)). This input parameter indicates the angle formed by the tangent direction to the absorber surface at the edge point (blue point at Fig. 1(a) where the concentrated radiation flux profile starts) and the ray intersecting at this point of the absorber. This angle is a relevant input parameter because it has a clear influence on the intercept factor ( $\gamma$ ). The closer  $\Psi$  is to  $\pi/2$  the more tolerant this reflector design will be to the absorber displacements or it is more probable that the sunshape profile tail rays reach it.

It is required to know where the algorithm is starting. We need to calculate the point where the first segment edge of the reflector is located. To get it, a reverse ray is launched from the edge of the concentrated profile (blue point in Fig. 1(b)). After taking into account the effects of refraction through the glass envelope we get the intersection of this ray with the coordinate ( $x=W$ ). It is convenient to note that all reflector geometries have to fulfill this condition because the global amount of energy concentrated is the same (once a specific objective profile is provided). In other words, the aperture length for all possible solutions is the same and is related to the whole integral of the objective profile, so the objective flux profile will indicate the value of  $W$ , pointing where the reflector initial point is located ( $x_0, y_0$ ).

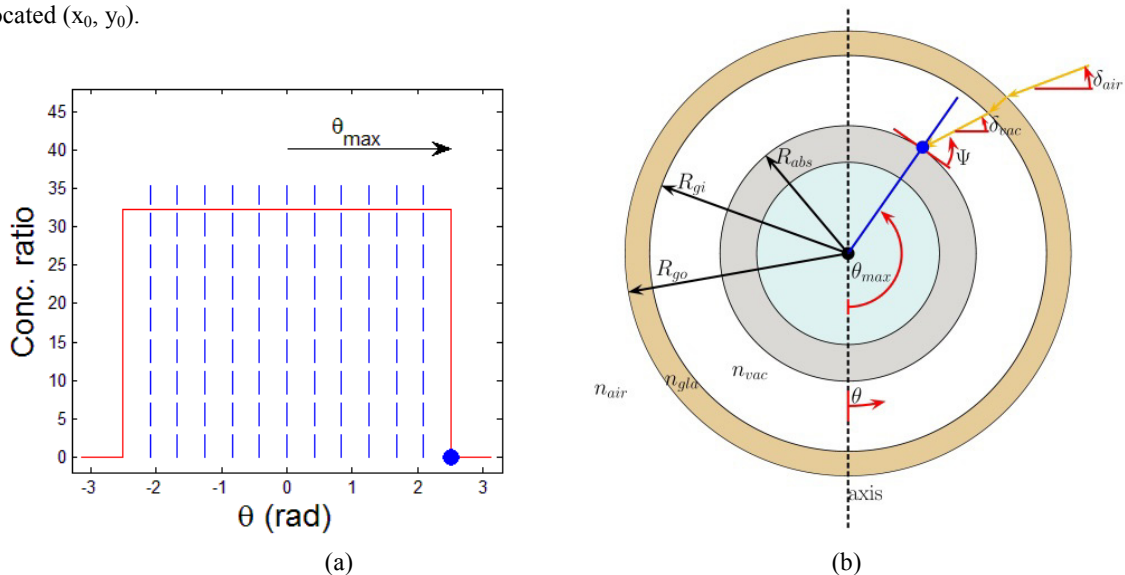


Fig. 1. (a) Objective profile for  $\theta_{max}=0.8\pi$ ; (b) Method starting.

The reflector geometry obtained is a set of  $N+1$  point, so the objective profile should be divided into  $N$  parts, setting a relation between every reflector segment and every division in the concentrated flux profile. The method consists of considering a system of non-linear equations for every reflector segment. This system provides the

coordinates of the next point  $(x_{n+1}, y_{n+1})$  from the previous one  $(x_n, y_n)$ . It states basically that the energy contained in the  $n$ th portion of the concentrated flux profile is the same that the whole amount of energy reflected by the  $n$ th segment of the reflector. Apart from this energy condition, an additional geometrical condition must be fulfilled. As it can be seen in Fig. 2, the incident ray onto the central point of the reflector segment, have to reach the absorber at the central point of the  $n$ th division in the flux profile, after considering the envelope refraction. The key question here is about the angle of the incident ray onto the  $n$ th reflector segment  $\phi_n$ . This fact is closely related to the solar sunshape profile. Nevertheless in this first step all rays are considered to be perpendicular to the aperture plane, so  $\phi_n=0$ , disregarding the sunshape profile effects.

This method begins from the initial point  $(x_0, y_0)$  obtained from the two input parameters:  $\theta_{\max}$  and  $\Psi$ . Solving the first system of 16 equations we obtain the point  $(x_1, y_1)$ . Actually, it is an input for the next segment. The method keeps going on until all the  $N$  systems have been solved sequentially, providing one half of the symmetric reflector. The error accumulated after all the concatenated resolutions can be quantified checking how far is the value  $x_N$  from  $x=R_{\text{abs}}$  (not  $x=0$ , due to the absorber shadow). This error is generally a small fraction of the last segment length, validating the method and the numerical algorithm used to solve the system of equations.

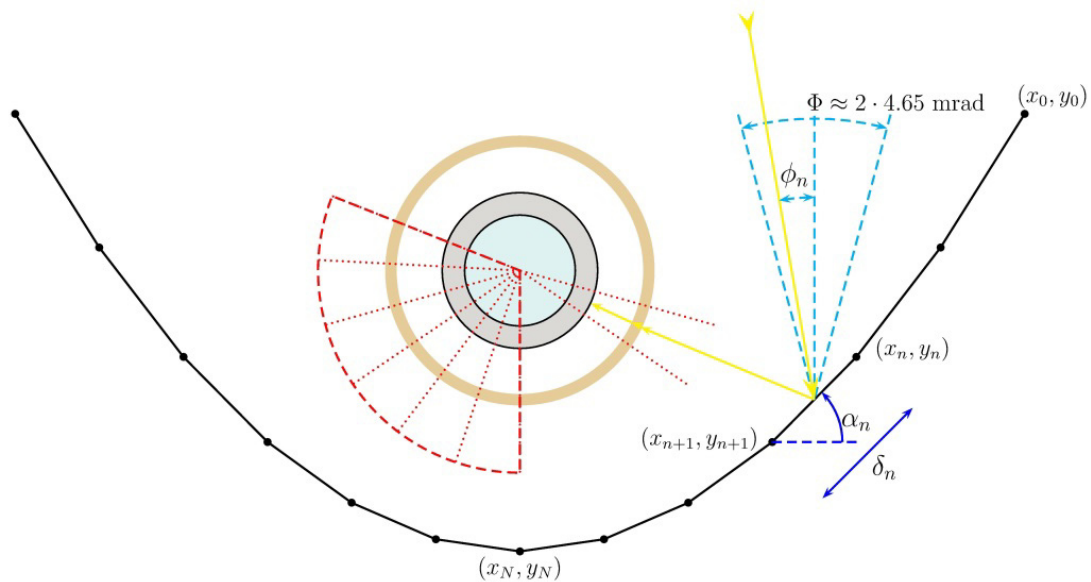


Fig. 2. Graphical description of the method.

## 2.2. Stage #2: Refinement process

As it might have been seen in the previous section, this method is not strictly speaking an IMCRT. Actually, it cannot be guaranteed that there exists a solution for any desired objective profile. The contribution of every reflector point to the concentrated radiation flux profile around the absorber tube is a particular distribution whose shape depends on the position of this reflector point respect to the absorber. So, the resulting profile is the addition of

many different distributions (slightly similar to the Gaussian profile). Then it cannot be guaranteed that the addition of different distributions provides any required global distribution.

This fact is observed in Fig. 3, where the resulting profile after following the first step (black line) is not exactly the objective profile. This is a consequence of the sunshape profile, due to the fact that we assumed initially that all rays reaching the reflector were normal to its aperture plane. There is no way of carrying out the strategy followed in the method first step considering different incoming ray directions in the same reflector segment, so we have taken the normal direction. This simplification is the responsible for this slight disagreement. The purpose of the second step is to correct as far as possible this discrepancy in order to move the solution closer to the objective profile.

The aim is to get a “smooth” function that provides the incoming ray angle deviation  $\phi_n$  for every reflector segment. In other words, we want to set a particular value for  $\phi_n$  in every reflector segment to correct the first stage solution. Once we have obtained this deviation function, we have to proceed again like in the first step, but including the new value of  $\phi_n$  in the system of equations (instead of  $\phi_n=0$ ), obtaining the corrected reflector geometry. This dual-step process can be repeated to keep improving the reflector geometry iteratively.

This deviation function proposed is not a unique optimum correction. Instead, this correction is obtained after a non-linear optimization problem where the objective functions can respond to several requirements. For example, we would prefer to obtain a sharper slope in the constant concentrated flux distribution without being really worried about slight fluctuations in the flat region. Otherwise, we might need a perfect planar flux distribution in the central part of the profile allowing a smooth decay at both edges. Anyway, we can adopt an alternative option finding a compromise solution considering both conditions. This is the strategy followed to obtain the final solution proposed in Fig. 3 (green line). Edges have been got narrower, enclosing more concentrating radiation inside the objective profile (red color).

### 3. Results and comparison with the Eurotrough (LS-3) collector design

#### 3.1. Concentrated radiation flux profiles

Results displayed here, correspond to a particular constant radiation flux profile case in which  $\theta_{\max}=0.8\pi$  and the intersection angle of the last ray is  $\Psi=0.35\pi$ . In Fig. 3 a comparison between the flux profiles considered in different stages of the method are depicted. The objective profile (red line) according to the input parameter ( $\theta_{\max}$ ) is approximated by means of the method first stage solution (black line). This preliminary solution shows a wide flat region in the center of the flux profile, but with the inconvenience of having considerable “smooth” edges, where a certain fraction of the concentrated radiation is out if the angular range  $-\theta_{\max} < \theta < \theta_{\max}$ . In order to reduce it, without penalizing considerably the constant distribution in the central part of the profile, a deviation function  $\phi_n$  solution has been found by means of an optimization strategy. As shown in Fig. 4, a continuous solution for  $\phi_n$  provides its corresponding value when solving the system of equations for every reflector segment in the second step. The reflector geometry obtained after this second stage provides the corrected concentrated flux profile depicted in Fig. 3 (green line). It shows “sharper” slopes, reducing the amount of concentrated radiation out of the objective profile and maintaining the constant tendency in the central region, with the exception of some slight fluctuations.

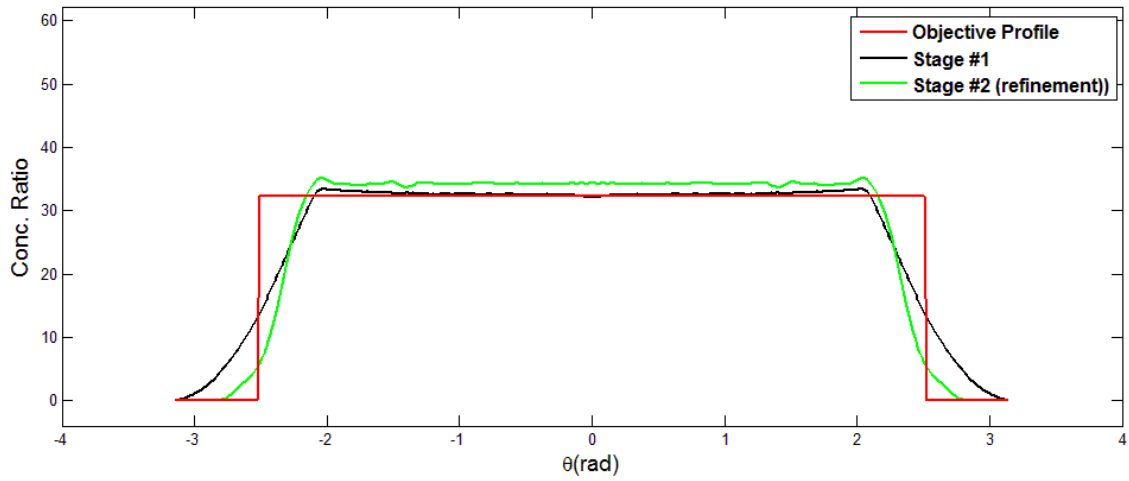


Fig. 3. Resulting concentrated radiation flux profiles in comparison with the objective profile.

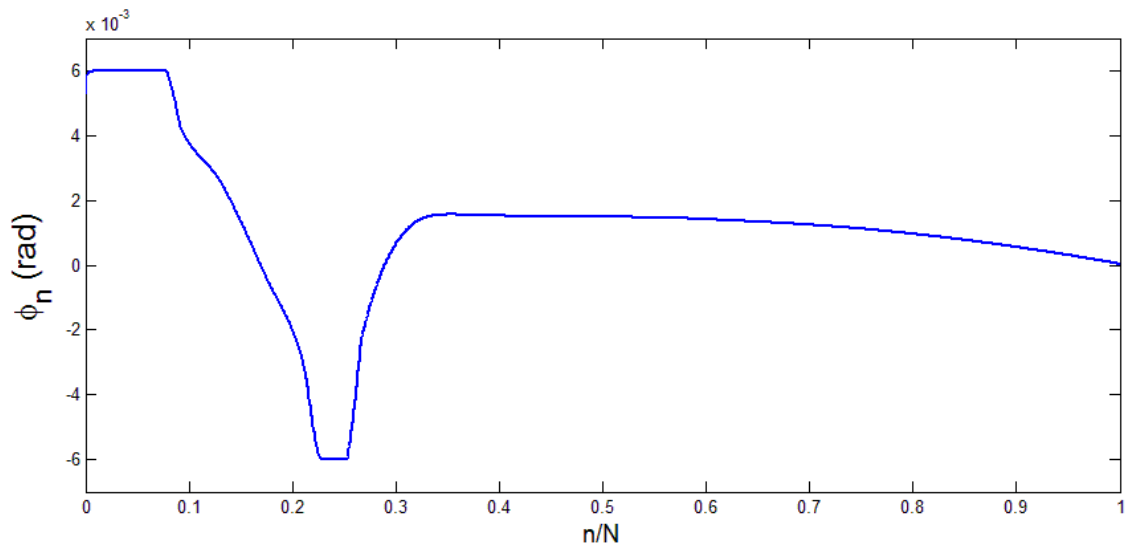


Fig. 4. Angular deviation  $\phi_n$  adopted in the reflector geometry correction.

### 3.2. Inputs parameters

In the context of this new method, aiming to get quasi-constant flux profiles onto round absorbers, there are only two free parameters (considering the EuroTrough collector aperture width and the absorber tube dimensions). These two values ( $\theta_{\max}$ ,  $\Psi$ ) have a clear influence on the characteristics of the resulting reflector geometry. The

“geometrical” quality of every reflector can be described through the intercept factor ( $\gamma$ ) that indicates the fraction of the reflected rays reaching the metallic absorber tube from a geometrical perspective. In this sense, it is also relevant to analyze how these input parameters affect to the reflector arc length obtained. A new parameter  $\Lambda$  is defined aiming to compare the reflector arc length respect to the Eurotrough design. The shorter the reflector is (maintaining obviously the same aperture width) the cheaper it is going to be. It is convenient to remark that results in this subsection correspond to those provided by the method first stage, without accomplishing the refinement process (second stage).

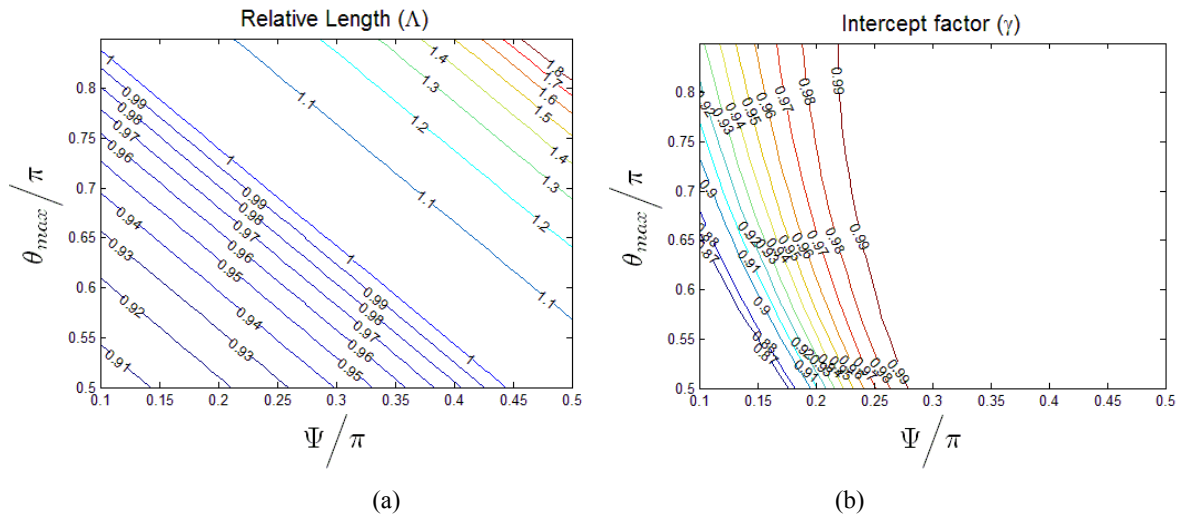


Fig. 5. (a) Relative length plane; (b) Interceptor factor dependence with the input parameters.

As seen on Fig. 5, the reduction of the reflector arc length evolves in the same direction respect to the intercept factor decrease. In other words, this means that getting a good concentrator (in the sense of good geometrical performance) requires spending more resources on longer reflector. Nevertheless, there exists a compromise region in which the intercept factor is above  $\gamma > 0.99$  and the parameter  $\theta_{max}$  is high enough to guarantee an acceptable homogeneous distribution around the absorber, achieving a shorter reflector respect to the reference ( $\Lambda < 1$ ). Anyway, these parameters value election depends on the requirements that the reflector must fulfill. If a shorter reflector is required without being concerned about the flux distribution around the absorber, we can locate the design point in the lower left region of the  $\Psi$ - $\theta_{max}$  plane.

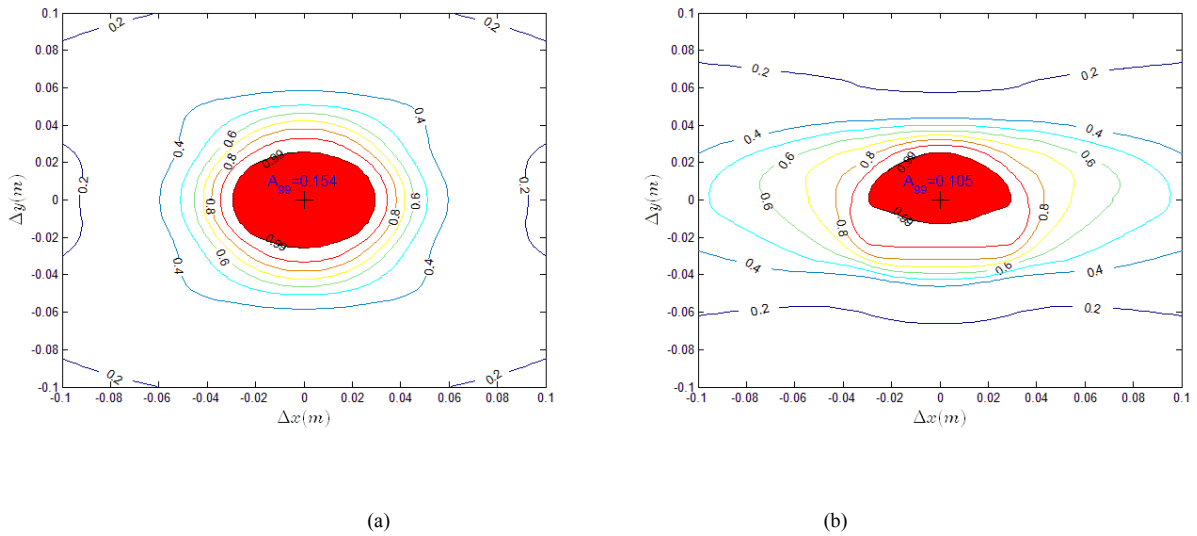


Fig. 6. (a) Geometrical performance plane for the standard Eurotrough concentrator; (b) Corresponding plane for the quasi-planar flux geometry after the stage #1 of the method ( $\theta_{\max}=0.8\pi$  and  $\Psi=0.35\pi$ ).

### 3.3. Geometrical performance plane

In PTC real applications absorber tube bending may occur. So it is convenient to study the tolerance of specific reflector geometry to a two-dimensional displacement of the absorber tube center respect to the focal line. It basically consists of calculating the intercept factor value ( $\gamma$ ) in relation to a displacement of the absorber tube location. The absorber displacement is described by the  $\Delta x - \Delta y$  coordinates.

As depicted in Fig. 6, this new geometry (b) is more vulnerable to undesirable displacements of the absorber tube below the design location, being an important weak spot respect to the Eurotrough collector design (a). However, it is not more vulnerable to upwards or lateral displacements of the absorber. The red area corresponds to the displacement region of the absorber where the intercept factor remains higher than 99%. In this sense, a new parameter can be defined ( $A_{99}$ ), related to the area fulfilling higher efficiency over a certain threshold (99%) that will indicate a general tolerance for absorber tube displacements. This area is non-dimensionalised by the absorber cross sectional area. It is obvious that the higher the parameter  $\theta_{\max}$  is, the more vulnerable the reflector design is to downwards displacements because it reflects rays onto the upper arc of the absorber. Finally the same analysis has been performed for the refined reflector geometry after the method second step, according to the deviation function displayed in Fig. 4. The fact of redirecting the rays in the profile tail onto the angular range indicated by the objective profile, leads to an increase of the  $A_{99}$  parameter respect to the case before the refinement process. After this correction, downwards displacements are better tolerated. In other words, the tail rays, initially reflected onto the absorber arc where  $\theta > \theta_{\max}$  have been redirected to the region indicated by the object profile ( $\theta < \theta_{\max}$ ).



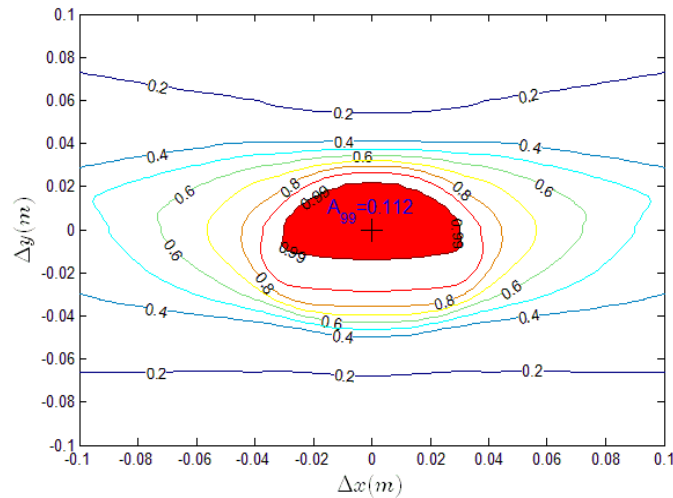


Fig. 7. Geometrical performance plane for a quasi-planar flux geometry (  $\theta_{\max}=0.8\pi$  and  $\Psi=0.35\pi$  ) after the refinement process (second step).

#### 4. Conclusions

A new proposed method provides the required line-focus solar reflector geometry in order to obtain a concentrated flux distribution on the solar collector receiver close to the initially profile desired (IMCRT). The method consists of two stages, the first allows an initial coarse solution and in the second stage a process of refinement of the solution is performed. The methodology proposed has been applied to modify the typical parabolic-trough geometry with absorber tubes, taking the Eurotrough collector design as a reference. Different solutions obtained from this method have been compared, paying special attention to the intercept factor ( $\gamma$ ) and the relative length respect to the Eurotrough geometry reference ( $\Lambda$ ) in relation with the two inputs parameters defined ( $\theta_{\max}$ ,  $\Psi$ ). Additionally, it has been proved the feasibility of refining the solution calculated in the first stage so as to compensate the sunshape profile effects.

#### Acknowledgements

This work has been developed under the framework of the project GEDIVA (ENE2011-24777) supported by the Spanish Department of Research, Development and Innovation, and of the European project STAGE-STE (ENERGY.2013.10.10, C.No. 609837) within the activity related to “Line-Focusing STE technologies”. First author thanks the Spanish government for granting his Ph.D. studies at the Plataforma Solar de Almeria (BES-2012-056876).

#### References

- [1] Esteban, A. Lüpfer, E. (2001), “Final Report EuroTrough project JOR3-CT98-0231”, public version.
- [2] Fernández-García A, Zarza E, Valenzuela L, Pérez M. Parabolic-trough solar collectors and their applications. *Renewable and Sustainable Energy Reviews*, 14(7); 2010. p. 1695 – 1721.
- [3] Lüpfer, E., Zarza-Moya, E., Geyer, M., Nava, P., Langenkamp, J., Schiel, W., Esteban, A., Osuna, R., Mandelberg, E. . EuroTrough collector qualification complete – Performance test results from PSA. ISES Solar World Congress 2003, Goteborg, Sweden.
- [4] Zarza E, Valenzuela L, León J, Hennecke K, Eck M, Weyers H, Eickhoff M. Direct steam generation in parabolic troughs: Final results and conclusions of the DISS project. *Energy*, 29, 2004. p. 635-644.
- [5] Mittelman G, Kribus A, Dayan A. Solar cooling with concentrating photovoltaic/thermal (CPVT) systems. *Energy Conversion and Management*, 48(9); September 2007. p. 2481-2490.
- [6] Evans D. On the performance of cylindrical parabolic solar concentrators with flat absorbers. *Solar Energy*, 19; 1977. p. 379 – 385.

- [7] Kok-Keong Chong, Sing-Liong Lau, Tiong-Keat Yew, Philip Chee-Lin Tan. Design and development in optics of concentrator photovoltaic system. *Renewable and Sustainable Energy Reviews*, 19; 2013. p. 598-612.
- [9] Mojiri A, Stanley C, Rosengarten G. Spectrally Splitting Hybrid Photovoltaic/thermal Receiver Design for a Linear Concentrator. *Energy Procedia*, 48; 2014. p. 618 – 627.
- [9] Sun Y, Wang Y, Zhu L, Yin B, Xiang H, Huang Q. Direct liquid-immersion cooling of concentrator silicon solar cells in a linear concentrating photovoltaic receiver. *Energy*, 65; 2014. p. 264 – 271.
- [10] Liu, Y., Hu, P., Zhang, Q., Chen, Z. Thermodynamic and optical analysis for a hybrid system with beam splitter and fully tracked linear Fresnel reflector concentrator utilizing sloped panels. *Solar Energy*, 103; 2014. P. 191-199.
- [11] Neumann A, Witzke A, Jones S, Schmitt G. Representative terrestrial solar brightness profiles. *J Sol Energ-T ASME* 2002; 124(2):198–204.